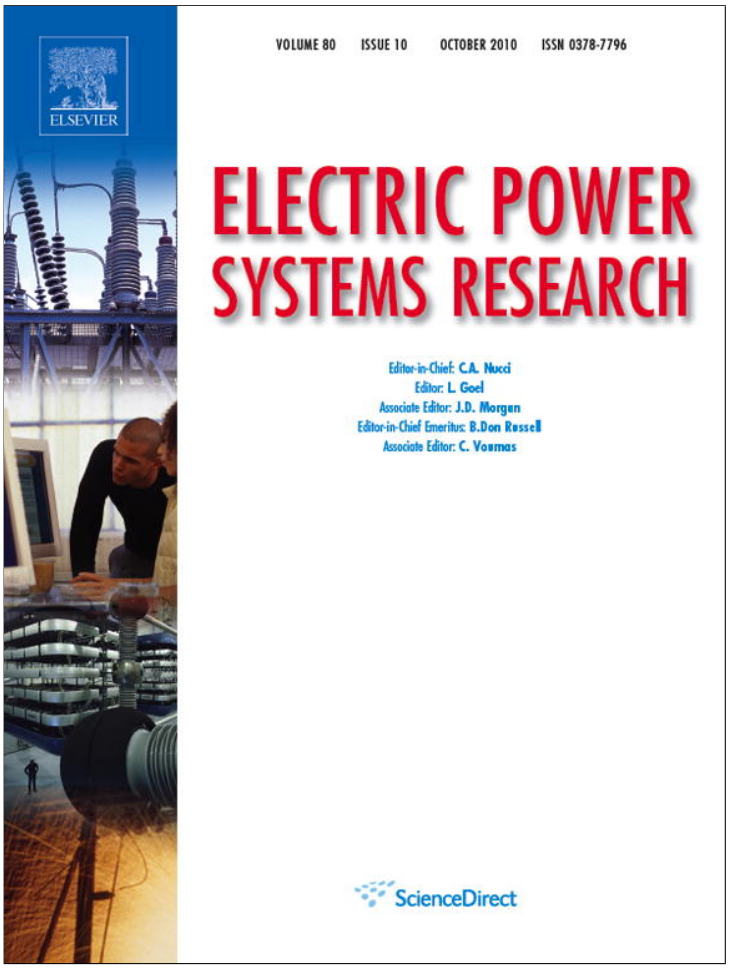

Electric Power Systems Research 80 (2010) 1267–1276

Contents lists available at ScienceDirect

Electric Power Systems Research

journal homepage: www.elsevier.com/locate/epsr

Allocation of reactive power support, active loss balancing and demand interruption ancillary services in MicroGrids

Mário Helder Gomes [a], João Tomé Saraiva [b,*]

[a] Departamento de Engenharia Electrotécnica, Instituto Politécnico de Tomar, Quinta do Contador, Estrada da Serra, 2300 Tomar, Portugal
[b] INESC Porto and Faculdade de Engenharia da Universidade do Porto, Campus da FEUP, Rua Dr. Roberto Frias, 4200 – 465 Porto, Portugal

ARTICLE INFO

Article history:
Received 11 December 2009
Accepted 29 April 2010
Available online 31 May 2010

Keywords:
MicroGrids
Electricity markets
Ancillary services
Reactive power/voltage control
Active loss balancing
Load curtailment

ABSTRACT

MicroGrids represent a new paradigm for the operation of distribution systems and there are several advantages as well as challenges regarding their development. One of the advantages is related with the participation of MicroGrid agents in electricity markets and in the provision of ancillary services. This paper describes two optimization models to allocate three ancillary services among MicroGrid agents – reactive power/voltage control, active loss balancing and demand interruption. These models assume that MicroGrid agents participate in the day-ahead market sending their bids to the MicroGrid Central Controller, MGCC, that acts as an interface with the Market Operator. Once the Market Operator returns the economic dispatch of the MicroGrid agents, the MGCC checks its technical feasibility (namely voltage magnitude and branch flow limits) and activates an adjustment market to change the initial schedule and to allocate these three ancillary services. One of the models has crisp nature considering that voltage and branch flow limits are rigid while the second one admits that voltage and branch flow limits are modeled in a soft way using Fuzzy Set concepts. Finally, the paper illustrates the application of these models with a Case Study using a 55 node MV/LV network.

1. Introduction

MicroGrids emerged in recent years as a very promising concept to allow wide spreading small generation sources namely in low voltage networks together with the incorporation of control devices associated both to small generation sources and low voltage loads [1–4]. This means that a MicroGrid can be seen as an association of a low voltage network with a number of components, as illustrated in Fig. 1. These components include loads, small scale generation devices (as small turbines, fuel cells, PV panels and wind turbines), storage devices (as flywheels, capacitors and batteries) and control devices. These control devices are associated with the micro-sources – MC controllers, with the controllable loads – LC controllers as well as with the MicroGrid Central Controller – MGCC, located in the beginning of the LV feeder [5]. According to this architecture, the MGCC acts as an interface both with the upstream Distribution Management System, DMS, of the Distribution Network Operator, DNO, and with the downstream Micro-source and Load Controllers – MC and LC.

As mentioned above, MicroGrids are contributing to change the still dominant paradigms associated with distribution network operation and with distributed generation. Distribution networks, namely LV networks, will no longer be passive ones but will incorporate a number of small sources getting generation closer to the demand and so contributing to turn the demand more aware of generation issues. On the other hand, the incorporation of control devices allows these small sources to provide a number of services upon request of the MGCC or of the upstream DMS system. This means that networks will have a larger amount of resources, not only in terms of providing energy but also in terms of different types of ancillary services. Regarding the demand, the incorporation of control devices can induce its participation in electricity markets, contributing to create more efficient mechanisms to profit from some demand elasticity as well as to enlarge the use of interruptible loads, provided that they receive an adequate remuneration. This means that the association of an LV network with small generation sources, loads and control devices can prove to be very powerful and effective in modernizing distribution networks and in integrating small scale distributed generation in a more natural way in power systems. Ultimately, MicroGrids can contribute to pass from the connection of large amounts of volatile DG paid in several countries according to subsidized feed-in tariffs to a more reasonable and natural way of integration while creating the conditions for their participation in markets and contributing to provide several services.

According to several authors [5,6], the development of MicroGrids brings several advantages to power systems namely the ones related with operation and investment issues, environmental

* Corresponding author. Tel.: +351 22 2094230; fax: +351 22 2094150.
E-mail addresses: mgomes@ipt.pt (M.H. Gomes), jsaraiva@fe.up.pt (J.T. Saraiva).

0378-7796/$ – see front matter © 2010 Elsevier B.V. All rights reserved.
doi:10.1016/j.epsr.2010.04.013

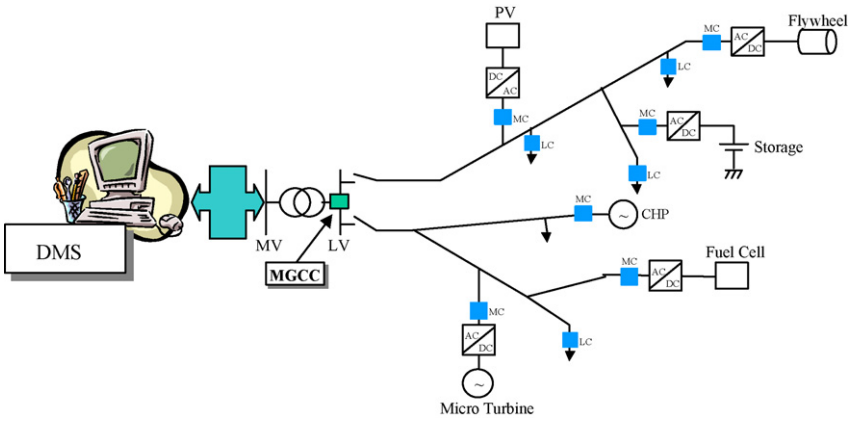

Fig. 1. Illustrative scheme of a MicroGrid.

issues, power quality improvement (namely reducing interruptions if operation in an isolated mode is considered [5,7,8]) and market issues (enabling the participation of MicroGrid agents in markets to provide electricity and services).

Although these advantages were identified in early publications on MicroGrids, their development and widespread still face a number of challenges related with the cost of generation technologies, with the development of control devices and new applications and models to allow the efficient and integrated operation of the MicroGrid and the upper stream networks, the absence of standards and, finally, the absence or still under developed legal and/or regulatory provisions to frame their installation and operation.

Given the advantages of MicroGrids and the new paradigm associated with their development, INESC Porto participated in two EU financed projects (MICROGRIDS and MORE MICROGRIDS projects) aiming at making new advances in several aspects associated with MicroGrid modeling. This paper describes part of the research developed in INESC Porto to allow increasing the participation of MicroGrid agents, namely small generation sources and loads, in the provision of some ancillary services. In this paper we will focus on the allocation of reactive power, on the allocation of active power generation to contribute to balance active losses and on the allocation of load interruption capability. Apart from this introductory section, this paper is structured as follows. Section 2 describes some approaches available to allow the participation of MicroGrid agents in markets and Section 3 describes the two developed mathematical, one of them corresponding to a crisp formulation and the second one using Fuzzy Set concepts to model soft constraints. Section 4 describes the solution algorithm implemented to solve these optimization problems and Section 5 illustrates the application of these models with a Case Study based on a 55 node MicroGrid. Finally, Section 6 draws the most relevant conclusions.

2. Overview of approaches to allocate ancillary services in MicroGrids

Among other advantages of MicroGrids, the creation of conditions to increase the participation of small generation sources and loads in electricity markets and the provision of some ancillary services are considered as most desirable in early publications on this subject, as [4,5], although several problems turn this integration difficult. Apart from other considerations, increasing the participation of small generation sources in MicroGrids will allow treating these generation facilities in a more natural way, substituting feed-in tariffs that, in several countries, represent increasing percentages of the final end user tariffs.

On the other hand, demand should be also more integrated in electricity markets [4,5] because it typically shows a very passive and inelastic behaviour so that current market implementations are, in practice, very asymmetrical. Introducing control devices namely in the MicroGrid loads and innovating in terms of remunerating the demand if it admits interruptions can correspond to a breakthrough to change its behaviour and to turn electricity markets more symmetric. This fact, together with the larger number of generation agents, will contribute to reduce the market power that today large generation companies still have.

In line with these concerns, reference [9] proposes an overall procedure to allow the participation of MicroGrid agents in electricity markets. This procedure corresponds to a symmetric assignment problem and once this auction ends all MicroGrid agents adjusted their positions in order to maximize their profits. The main grid is also considered a buying or selling agent so that it is possible to buy power from it to supply the MicroGrid demand, as well as selling power to the upward voltage network.

Afterwards, reference [10] describes an Energy Management System, EMS, based on the use of neural networks to implement a number of functions to autonomously adopt decisions regarding the dispatch of the generators in the MicroGrid aiming at minimizing the global energy cost. References [11,12] describe agent-based approaches to model MicroGrids. As an example, the agent-based platform detailed in [11] includes agents to model the MicroGrid Central Controller, the Micro-source Controllers and the Load Controllers. This agent platform was implemented on a laboratory micro grid using different storage schemes. Finally, [13] addresses the provision of some ancillary services. This reference focuses on the provision of primary reserve, although the authors indicate that the developed models and techniques can be extended to the secondary and tertiary reserves.

3. Allocation of reactive power, loss balancing and interruption services

3.1. General architecture and market cycle

In this paper we adopted a MicroGrid architecture similar to the one described in [5]. In this approach, the MicroGrid generation and load agents send selling and buying bids to the MicroGrid Central Controller, MGCC, that aggregates and communicates them to the Market Operator. In this sense, and apart from other functions, the MGCC acts as an interface between the MicroGrid agents and the Market Operator. The Market Operator runs an auction for the entire power system and determines the next day hourly economic schedule. Similarly to what occurs in transmission networks, the entity in charge of the MicroGrid operation checks the technical feasibility of these economic schedules, namely voltage magnitude and branch flow limits. In the MicroGrid, these functions

are assigned to the MGCC that, in this sense, acts as the MicroGrid System Operator. The MGCC should also assign some ancillary services as, for instance, reactive power/voltage control, balancing active losses and load curtailment resources. This scheme is implemented according to the following main steps:

- once the MGCC receives the economic schedule from the Market Operator, it runs an AC Power Flow to check for the technical feasibility of that schedule. This study is also used to obtain a complete first operation point of the MicroGrid that will be used in subsequent steps;
- then, the MGCC runs an adjustment market based on adjustment generator and load bids in order to compute the changes in this economic schedule to turn the operation point technically feasible, namely if there are voltage magnitude or branch flow violations. Even if such violations did not occur, this study is run to allocate generation to balance active losses and to assign reactive power;
- this study is done minimizing the adjustment cost resulting from accepting generator or load adjustment bids and the problem is subjected to a number of constraints, some them having a non-linear nature. This non-linear optimization problem was solved using a Sequential Linear Programming, SLP, algorithm that starts at the operation point previously identified, linearizes the non-linear constraints around this operation point, solves the linearized optimization problem, updates the injected powers and runs a new AC Power Flow study to update the operation point and to check for convergence;
- when the above iterative procedure converges, one gets the final schedule of the MicroGrid sources and loads, the nodal voltages and the active, reactive and apparent branch flows.

In the next paragraphs we will detail the modelization of the capability diagram of synchronous generators, since this information is used in the mentioned optimization problems, the generator and demand adjustment bids and the two developed optimization models, one of them having crisp nature and the other modeling voltage magnitude and branch flow limits as soft constraints using Fuzzy Set Theory concepts.

3.2. Synchronous generator capability diagram

The operation area of synchronous generators is delimited by several curves leading to a diagram as the one illustrated in Fig. 2. This means that active and reactive powers are coupled, that is, individual P and Q limit constraints are insufficient to represent accurately the operation of synchronous generators.

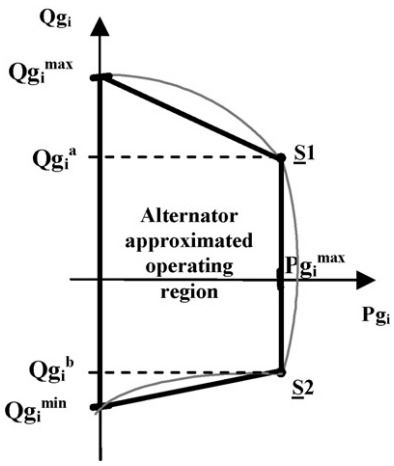

Fig. 2. Capability diagram of a synchronous generator.

The diagram sketched in Fig. 2 was modeled considering the following three curves:

- Curve 1, between $(0, Qg_i^{\max})$ and $(Pg_i^{\max}, Qg_i^{a})$, represents the rotor field current limit;
- Curve 2, from $\underline{S}_1$ to $\underline{S}_2$, is the armature limit. It can be represented by a vertical line often associated with the maximum output power of the primary machine;
- Curve 3, the arc between $(0, Qg_i^{\min})$ and $(Pg_i^{\max}, Qg_i^{b})$, represents the stability limit.

Admitting that $Pg_i^{\max}$, $Qg_i^{\max}$, $Qg_i^{\min}$, Qg_i^{a} and Qg_i^{b} are known, it is possible to obtain linear expressions to model these curves. These constraints will then be integrated in the optimization model used to check the feasibility of the economic dispatch because the P and Q outputs are not independent.

3.3. Generator and demand adjustment bids

As mentioned above, adjustment bids are used by MicroGrid generators and loads to transmit information about the changes on the active power scheduled by the Market Operator that they admit, together with the price they want to receive for these changes. Changes on the generation schedule may be due to the enforcement of operation constraints or to allow a reactive power output given that the P and Q values are coupled via the capability diagram. From a mathematical point of view these changes are represented by ΔPg_i^A variables that can assume both positive or negative values, implying in both cases the payment of an adjustment price, Cg_i^A. Apart from this adjustment price, these bids can also include an indication regarding the maximum variation, vg_i^{tol}, it is admitted regarding the base amount scheduled by the Market Operator.

The initial schedule of micro-sources can also change in order to allocate active power to balance active losses. These changes, all of them non negative, are represented by ΔPg_i^L variables. This means that the final schedule of generator i is given by (1), admitting that Pg_i^o represents the active power scheduled by the Market Operator.

$$Pg_i^{\text{final}} = Pg_i^o + \Delta Pg_i^A + \Delta Pg_i^L \quad (1)$$

Regarding the loads, they can play an important role in alleviating some constraints provided that they accept being interrupted if they are adequately remunerated for this service. Load adjustment bids include an adjustment price, Cd_j^A, together with the amount of load scheduled in the day-ahead market that one admits to curtail. This capability can be interpreted as an ancillary service provided to the MGCC turning the operation of the MicroGrid, and in fact of the whole system, more flexible. Mathematically, this is modeled by ΔPd_j^A variables, all of them non-positive. As a result, once the mentioned optimization problem is solved, the final scheduled loads are given by (2) assuming that Pd_j^o represents the demand initially scheduled by the Market Operator.

$$Pd_j^{\text{final}} = Pd_j^o + \Delta Pd_j^A \quad (2)$$

3.4. Model 1 – crisp optimization model

The initial optimization problem used to evaluate the technical feasibility of the Market Operator schedule was originally described in [14]. In this paper, this model is enhanced in order to allow computing the contribution of each generator to balance active losses, in the first place, and then to model voltage magnitude and branch flow limit constraints in a soft way, using Fuzzy Set Theory concepts. Regarding the first aspect, the linearized optimization

problem to be solved in each iteration of the market cycle detailed in Section 3.1 is given by (3)–(16) admitting that the network under analysis has *Ng* generators, *Nd* loads and *Nb* branches.

$$\text{Min } Z = \rho^{MO} \times \sum_{i=1}^{Ng} \Delta Pg_i^L + \sum_{i=1}^{Ng} \left|\Delta Pg_i^A\right| \times Cg_i^A + \sum_{j=1}^{Nd} \left|\Delta Pd_j^A\right| \times Cd_j^A \quad (3)$$

$$\text{Subject to : } \Delta V_i^{\min} \le \Delta V_i \le \Delta V_i^{\max} \quad (4)$$

$$\Delta\theta_{ij}^{\min} \le \Delta\theta_{ij} \le \Delta\theta_{ij}^{\max} \quad (5)$$

$$0 \le \Delta Pg_i^L \le \Delta Pg_i^{L\max} \quad (6)$$

$$-\frac{vg_i^{\text{tol}}}{100} \times Pg_i^o \le \Delta Pg_i^A \le \frac{vg_i^{\text{tol}}}{100} \times Pg_i^o \quad (7)$$

$$0 \le \Delta Pg_i^A \le \frac{vg_i^{\text{tol}}}{100} \times Pg_i^{\max} \quad (8)$$

$$\Delta Pg_i^{\min} \le \Delta Pg_i^A + \Delta Pg_i^L \le \Delta Pg_i^{\max} \quad (9)$$

$$-Pd_j^o \le \Delta Pd_j^A \le 0 \quad (10)$$

$$Qg_i^o + \Delta Qg_i \ge Qg_i^{\min} + \frac{Qg_i^b - Qg_i^{\min}}{Pg_i^{\max}} \times (Pg_i^o + \Delta Pg_i^A + \Delta Pg_i^L) \quad (11)$$

$$Qg_i^o + \Delta Qg_i \le Qg_i^{\max} - \frac{Qg_i^{\max} - Qg_i^a}{Pg_i^{\max}} \times (Pg_i^o + \Delta Pg_i^A + \Delta Pg_i^L) \quad (12)$$

$$\sum_{k=1}^{Nb} \Delta P_k^{\text{loss}}(\Delta V, \Delta\theta) = \sum_{i=1}^{Ng} \Delta Pg_i^L \quad (13)$$

$$\Delta P_i^{inj}(\Delta V, \Delta\theta) = (\Delta Pg_i^A + \Delta Pg_i^L) - \Delta Pd_i^A \quad (14)$$

$$\Delta Q_i^{inj}(\Delta V, \Delta\theta) = \Delta Qg_i - \Delta Qd_i \quad (15)$$

$$\Delta S_{ij}^{\min} \le \Delta S_{ij}(\Delta V, \Delta\theta) \le \Delta S_{ij}^{\max} \quad (16)$$

The objective function (3) incorporates the following three terms:

- the first term corresponds to the cost of generating power to balance active losses in the MicroGrid. This cost is obtained multiplying the addition of the ΔPg_i^L variables by the market energy price, ρ^{MO}, obtained by the Market Operator in the auction conducted to obtain the initial economic schedule;
- the second term represents the cost of using generator adjustment bids and it corresponds to the multiplication of the generation adjustment variables ΔPg_i^A by the respective adjustment cost Cg_i^A;
- similarly, the third term represents the demand adjustment cost and it is obtained multiplying the load adjustment variables, ΔPd_j^A, by the corresponding adjustment cost Cd_j^A.

This objective function is subjected to the following constraints:

- constraints (4) and (5) impose the minimum and maximum limits on the nodal voltage magnitude variations and on the phase difference between pairs of nodes;
- constraints (6)–(9) represent the ranges of the ΔPg_i^L and ΔPg_i^A adjustment variables. Constraint (6) limits the contribution of each generator to balance active losses and (7) and (8) impose limits on the generation adjustments required to enforce technical or operational constraints. Constraint (9) establishes the limits for the addition of ΔPg_i^L and ΔPg_i^A;
- constraint (10) defines the range of active power demand adjustments, all of them non-positive;
- constraints (11) and (12) model the lower and the upper curves in Fig. 2 representing the synchronous generator capability diagram;
- constraint (13) balances the branch active power losses computed using voltage magnitude and phase variations with the active power losses assigned to each generator, modeled by the ΔPg_i^L variables. The branch active power loss deviations are computed using a linearized expression that is obtained using the linear terms of the Taylor Series of the exact active power losses expression. The values of the partial derivatives regarding voltage magnitudes and phases are computed using the operation point obtained by the AC Power Flow study, in the scope of the SLP iterative process;
- constraints (14) and (15) represent linearized versions of the active and reactive injected power equations. These linearized expressions also correspond to the linear terms of the Taylor Series of the full AC injected power expressions;
- finally, constraint (16) imposes the range of the apparent power in each branch *ij*. Once again, they are established using the linear terms of the Taylor Series of the full AC apparent power flow in branch *ij*.

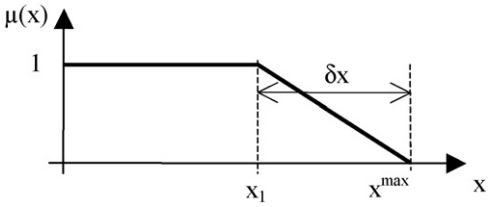

Fig. 3. Membership function of the maximum limit of a variable *x*.

3.5. Fuzzy Linear Programming model

3.5.1. Soft limits

Some operation limits allow some degree of violation without placing immediate problems for system operation. Some grid codes establishing the rules for system operation already admit larger than normal branch flow limits provided that these operation situations are limited in time. This suggests representing voltage and branch flow constraints using Fuzzy Sets [15] as detailed below. A Fuzzy Set can be interpreted as a generalization of a traditional crisp set in the sense that in crisp sets an element fully belongs or completely does not belong to a set, that is, we only admit the 1 and the 0 logic values. In Fuzzy Sets we can assign to each element a degree of membership in the interval [0,1] expressing the compatibility of that element to the definition of the set. This means that a Fuzzy Set $\tilde{A}$ can be seen as a set of ordered pairs (17) in which the first element in each pair is an element x of the universe X under analysis and the second, $\mu_{\tilde{A}}(x)$, is the degree of membership of x to $\tilde{A}$.

$$\tilde{A} = \{(x, \mu_{\tilde{A}}(x)), x \in X\} \quad (17)$$

Using these concepts, the limit of a branch flow is modeled in terms of a crisp value x_1 together with a tolerance δx as illustrated in Fig. 3. According to this figure, the membership function of the flow x is 1 if it is not larger than x_1. From x_1 to $x^{\max}$ the membership

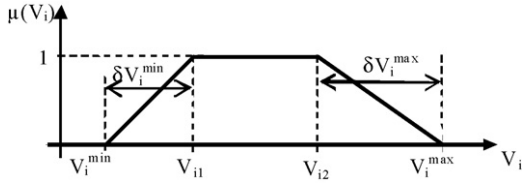

Fig. 4. Membership function of the voltage magnitude in node *i*.

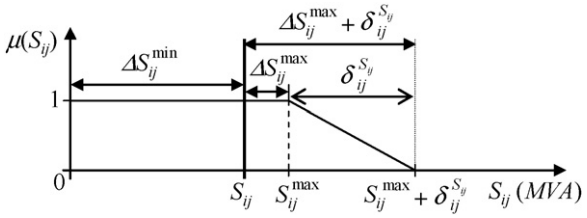

Fig. 5. Fuzzy membership function of the apparent power in branch *ij*.

level decreases to 0. This function is modeled by (18).

$$\mu(x) = \begin{cases} 1 & \text{if } x \le x_1 \\ [0;1[& \text{if } x_1 < x \le x^{\max} \\ 0 & \text{if } x \ge x^{\max} \end{cases} \quad (18)$$

In a similar way, Fig. 4 represents the membership function of the voltage in node *i*. Voltages from V_{i1} to V_{i2} have the maximum membership degree, 1. Voltages lower than V_{i1} or higher than V_{i2} can be still accepted but their membership values decrease from 1 to 0. Expression (19) models this fuzzy membership function.

$$\mu(V_i) = \begin{cases} 1 & \text{if } V_{i1} \le V_i \le V_{i2} \\ [0;1[& \text{if } V_i^{\min} \le V_i < V_{i1} \text{ or } V_{i2} < V_i \le V_i^{\max} \\ 0 & \text{if } V_i < V_i^{\min} \text{ or } V_i > V_i^{\max} \end{cases} \quad (19)$$

3.5.2. Model 2 – Fuzzy Linear Programming model

Once the Market Operator initial purely economic schedule is obtained, the MGCC acting as the MicroGrid system operator solves the problem (20)–(35) aiming at maximizing the satisfaction degree μ related with the membership function of the soft constraints and with the objective function of the original crisp problem given by (3). Using a formulation similar to the one detailed for the soft constraints, the objective function (3) of the original crisp problem is converted in constraint (21) in which FO^{des} is the largest value that the objective function of the original problem can assume still having the satisfaction degree of 1 and δ^{FO} is the admitted tolerance. This means that when the value of *FO* increases from FO^{des} to $FO^{\text{des}} + \delta^{FO}$, its membership degree decreases from 1 to 0, which is in line with the graphical representation in Fig. 3.

$$\text{Max } Z = \mu \quad (20)$$

$$\text{Subject to : } \; FO + \mu \times \delta^{FO} \le FO^{\text{des}} + \delta^{FO} \quad (21)$$

$$\Delta V_i - \mu \times \delta^{V\min} \ge \Delta V_i^{\min} - \delta^{V\min} \quad (22)$$

$$\Delta V_i + \mu \times \delta^{V\max} \ge \Delta V_i^{\max} + \delta^{V\max} \quad (23)$$

$$\Delta\theta_{ij}^{\min} \le \Delta\theta_{ij} \le \Delta\theta_{ij}^{\max} \quad (24)$$

$$\Delta Pg_i^{\min} \le \Delta Pg_i^A + \Delta Pg_i^L \le \Delta Pg_i^{\max} \quad (25)$$

$$-\frac{vg_i^{\text{tol}}}{100} \times Pg_i^o \le \Delta Pg_i^A \le \frac{vg_i^{\text{tol}}}{100} \times Pg_i^o \quad (26)$$

$$0 \le \Delta Pg_i^A \le \frac{vg_i^{\text{tol}}}{100} \times Pg_i^{\max} \quad (27)$$

$$-Pd_j^o \le \Delta Pd_j^A \le 0 \quad (28)$$

$$Qg_i^o + \Delta Qg_i \ge Qg_i^{\min} + \frac{Qg_i^b - Qg_i^{\min}}{Pg_i^{\max}} \times (Pg_i^o + \Delta Pg_i^A + \Delta Pg_i^L) \quad (29)$$

$$Qg_i^o + \Delta Qg_i \le Qg_i^{\max} - \frac{Qg_i^{\max} - Qg_i^a}{Pg_i^{\max}} \times (Pg_i^o + \Delta Pg_i^A + \Delta Pg_i^L) \quad (30)$$

$$\sum_{k=1}^{Nb} \Delta P_k^{\text{loss}}(\Delta V, \Delta\theta) = \sum_{i=1}^{Ng} \Delta Pg_i^L \quad (31)$$

$$\Delta P_i^{inj}(\Delta V, \Delta\theta) = (\Delta Pg_i^A + \Delta Pg_i^L) - \Delta Pd_i^A \quad (32)$$

$$\Delta Q_i^{inj}(\Delta V, \Delta\theta) = \Delta Qg_i - \Delta Qd_i \quad (33)$$

$$\Delta S_{ij}(\Delta V, \Delta\theta) + \mu \times \delta_{ij}^{Sij} \le \Delta S_{ij}^{\max} + \delta_{ij}^{Sij} \quad (34)$$

$$0 \le \mu \le 1 \quad (35)$$

In this formulation constraints (22) and (23) represent the minimum and maximum limits of the voltage magnitudes admitting tolerances $\delta^{V\min}$ and $\delta^{V\max}$, constraint (24) imposes limits to the phase differences and (25)–(27) impose the limits for the generator ΔPg_i^L and ΔPg_i^A variables. Constraint (28) imposes the limits on load curtailment and constraints (29) and (30) correspond to the linearized lower and upper curves of the capability diagram sketched in Fig. 2. Constraints (31)–(33) have the same meaning already detailed for Model 1 described in Section 3.4. Constraint (34) represents the fuzzified version of the maximum limit of the apparent power flow in branch *ij* admitting the tolerance δ_{ij}^{Sij}, as sketched in Fig. 5. Finally, constraint (35) specifies the range of the membership degree μ in the interval [0,1].

4. Solution algorithm – Sequential Linear Programming, SLP, approach

The operation cycle starts with the communication to the MGCC of the buying and selling bids by all demand and generation agents in the MicroGrid. The MGCC aggregates all these bids and conveys this information to the Market Operator. Once the Market Operator runs the auction for each trading period of the next day, it communicates to the MGCC the accepted buying and selling bids of the MicroGrid agents. Then the MGCC uses this information to check for the technical feasibility of this economic schedule namely running an AC Power Flow. Based on the operation point identified with this study, the AC Power Flow equations and the branch apparent power flow limit constraints are linearized and it is run the optimization problem (3)–(16), in case of the crisp optimization formulation, and the problem (20)–(35) regarding the fuzzy approach.

Taking the fuzzy approach as an example, the iterative solution algorithm proceeds as follows. After solving the optimization problem, one obtains the deviations of the active and reactive generations and demands as well as the deviations of the voltage magnitudes. This allows running a new AC Power Flow study to update the operation point, linearizing again the non-linear constraints and running again the optimization problem. The convergence of this iterative process is evaluated comparing the absolute value of the deviations of voltage magnitudes, phases and active and reactive powers at the end of each iteration with specified tolerances. When the absolute value of all these deviations is smaller than specified tolerances, we get the solution for the non-linear problem. If convergence was not yet reached, the process gets back in order to run a new power flow, to linearize again the non-linear constraints and to solve again the linearized optimization problem.

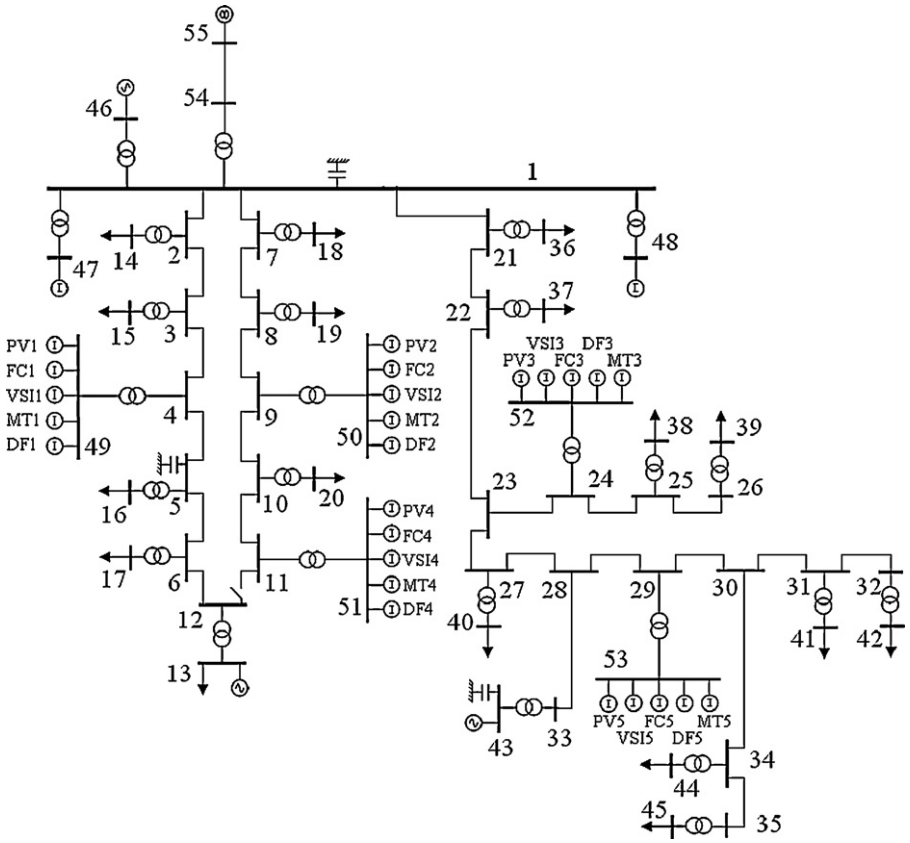

Fig. 6. Scheme of the 55 node MV/LV test network.

5. Case study

5.1. System data

The developed models and the described solution algorithm were tested using the 55 node MV/LV network presented in Fig. 6 [16]. This MV/LV network is connected through node 55 to an upper level voltage network that is modeled by an equivalent generator, so that one can still consider situations in which part of the demand of this MV/LV network is supplied by the rest of the system. This network has small generation sources connected to nodes 13, 43 and 46–53. Tables 1 and 2 detail the data of this network. Table 1 includes generator selling bids, namely the maximum available power, the bid power and the generation bid price and the data to model the capability diagram of each generator, using the model described in Section 3.2, together with the generator adjustment price, Cg_i^A, and the maximum power each generator admits to change its initial schedule, νg_i^{tol}. Table 2 details the load buying bids and the corresponding adjustment price, Cd_j^A. The branch data [16] can be obtained on request from the authors.

This network includes three capacitor banks connected to nodes 1, 5 and 43. The capacitor in node 1 has 2.0 Mvar, the one in node 5 has 0.5 Mvar, and the capacitor bank in node 43 has 0.5 Mvar. Finally, the voltage magnitude limits were set at 0.97 and 1.03 pu.

5.2. Initial Market Operator schedule

As indicated in the operation cycle detailed in Section 3.1, the buying and selling bids are sent to the Market Operator that runs an uniform price auction, ordering the selling bids by the ascending order of the bid price and the buying bids by the descending order of the bid price. Using this auction, it is obtained the market clearing price and the accepted buying and selling bids. Let us admit that the generation and demand purely economic schedule corresponds to the powers indicated in Table 3 and that the market price, ρ^{MO}, is 40.8 €/MWh.

Table 1
Generator selling bids, data to model the capability diagram of the generators and adjustment bids.

bus i	Pg_i^{bid} MW	Cg_i^{bid} €/MWh	$Pg_i^{\max}$ MW	$Qg_i^{\max}$ Mvar	Qg_i^{a} Mvar	Qg_i^{b} Mvar	$Qg_i^{\min}$ Mvar	νg_i^{tol} %	Cg_i^{A} €/MWh
13	0.40	16.0	0.40	0.50	0.50	−0.50	−0.50	100	160.0
43	1.50	16.0	1.50	1.00	1.00	−0.50	−0.50	100	160.0
46	0.70	16.0	0.70	0.50	0.50	−0.50	−0.50	100	120.0
47	0.10	60.0	0.10	0.01	0.01	−0.01	−0.01	100	144.0
48	0.80	24.0	0.80	0.30	0.30	−0.30	−0.30	100	80.0
49	0.25	32.0	0.25	0.10	0.10	−0.10	−0.10	100	80.0
50	0.25	24.0	0.25	0.10	0.10	−0.10	−0.10	100	80.0
51	0.25	28.0	0.25	0.10	0.10	−0.10	−0.10	100	80.0
52	0.25	32.0	0.25	0.10	0.10	−0.10	−0.10	100	80.0
53	0.25	16.0	0.25	0.10	0.10	−0.10	−0.10	100	80.0
55	7.00	40.8	7.00	2.50	2.50	−2.50	−2.50	20	80.0

Table 2
Buying and adjustment bids of loads.

bus i	Pd_i^{bid} MW	Qd_i Mvar	Cd_j^{bid} €/MWh	Cd_j^A €/MWh
13	0.900	0.436	48.0	304.0
14	0.838	0.275	41.6	312.0
15	0.838	0.275	44.0	336.0
16	0.419	0.138	42.4	320.0
17	0.419	0.138	43.2	352.0
18	0.838	0.275	48.0	368.0
19	0.838	0.275	64.0	352.0
20	0.419	0.138	56.0	328.0
36	0.216	0.105	48.0	312.0
37	0.135	0.065	43.2	304.0
38	0.135	0.065	41.6	344.0
39	0.086	0.042	48.0	368.0
40	0.216	0.105	44.0	432.0
41	0.135	0.065	48.0	408.0
42	0.086	0.042	44.8	312.0
44	0.135	0.065	48.0	320.0
45	0.086	0.042	56.0	336.0

5.3. Case 1 – base demand – crisp approach

In the first place, we used Model 1 considering the demand indicated in Table 2 and the schedule obtained by the Market Operator in Table 3. In one simulation we considered that the breaker in branch 11–12 of Fig. 6 was opened and in other one that it was closed, namely to simulate an MV network in an urban area. In both cases, the network is operating well below its limits, namely in terms of voltage magnitudes and branch flows. This means that in both cases the ΔPg_i^A and the ΔPd_j^A variables are zero meaning that it not necessary to change the initial Market Operator schedule due to operation or security reasons. Regarding the ΔPg_i^L variables representing the contribution of each generator to balance branch losses, these variables are all zero except for node 47. When the breaker is opened this variable takes the value of 0.028 MW and when it is closed it assumes the value of 0.026 MW. This means that, in both cases, branch losses are balanced in a single node, node 47.

Table 3
Initial Market Operator schedule.

bus i	Pg_i MW	Pd_i MW
13	0.40	0.900
14	–	0.838
15	–	0.838
16	–	0.419
17	–	0.419
18	–	0.838
19	–	0.838
20	–	0.419
36	–	0.216
37	–	0.135
38	–	0.135
39	–	0.086
40	–	0.216
41	–	0.135
42	–	0.086
43	1.50	–
44	–	0.135
45	–	0.086
46	0.70	–
47	0	–
48	0.80	–
49	0.25	–
50	0.25	–
51	0.25	–
52	0.25	–
53	0.25	–
55	2.089	–

When the breaker is opened, the objective function has the value of 1.142 €/h and it is only due to the value of the generated power required to balance branch losses. This means that in terms of the objective function (3), the second and the third terms are zero and the value just mentioned results from multiplying the amount of losses (0.028 MW) by the market price, ρ^{MO}, that is by 40.8 €/MWh.

If Model 2 was used, we would have obtained the same operation point since for this load level there are no violations of voltage magnitude or branch flow crisp limits. This means that the tolerances admitted in the scope of the Fuzzy Linear Programming model would not be used.

5.4. Case 2 – results with demand increased by 30%

5.4.1. Results using model 1 – crisp approach

In this case, the two models were tested admitting that the load in all nodes was increased by 30% to get a more stressed operation situation. Fig. 7 and Table 4 detail the final solution obtained with Model 1 regarding voltage magnitudes and the final dispatch.

As indicated in Table 4 and differently from what occurred in Case 1, in this case the ΔPg_i^A variables for generators in nodes 46, 48, 52, 53 and 55 have negative values in the final dispatch. This means that the final dispatched powers of the generators in these nodes are more reduced regarding the initially scheduled values. Regarding the loads, the value obtained for the ΔPd_j^A variable in node 13 is −0.342 MW indicating there was load curtailment. This curtailment is explained because the apparent power flow in branch 1–2 rose in this case to 3.5 MVA (3.450 MW and 0.587 Mvar) due to the increase of the loads by 30% and this value corresponds to the limit specified for this flow. This prevents transmitting more power to the feeder supplying nodes 2–6, 12 and 13 so that the load connected to node 13 is curtailed by 0.342 MW.

In this case, branch losses are 0.035 MW and their compensation is distributed by nodes 47 and 55 as indicated in Table 4, regarding the values obtained for the ΔPg_i^L variables. Part of the power required to balance active losses internal to the MicroGrid is supplied by the upper level voltage network through node 55. On the other hand, the capacitors connected to nodes 1 and 5 generate 1.959 and 0.5 MVar, respectively.

The final value of the objective function is 133.76 €/h. This value is much larger than the values obtained for Case 1. This is explained by the use of adjustment bids both for the load in bus 13 and for the five generators mentioned above. This means that in the objective function (3) the three terms are now non-zero. The first one is associated with the power required to balance branch losses and it takes the value of 0.035 MW multiplied by the market price. The second term is associated with generation adjustments and it results from the multiplication of the values of the ΔPg_i^A variables obtained for nodes 46, 48, 52, 53 and 55 by the adjustment prices Cg_i^A in Table 1 for each of these nodes. The third term is associated with load curtailments and, in this case, it comes from multiplying the load curtailment in node 13, 0.342 MW, by the adjustment price for this node, that is by 304.0 €/MWh, as indicated in Table 2. The contribution of this third term in (3) is dominant since it assumes the value of 103.97 €/h out of the 133.76 €/h which means that the curtailment of load in node 13 is responsible for about 77% of the final value of the objective function.

Finally, Fig. 7 shows the voltage profile obtained for Case 2 – Model 1 indicating that voltages are constrained by the rigid limit of 1.03 pu. This graph shows that this crisp limit is reached for several nodes, namely for buses 33, 46 and 48–55.

5.4.2. Results using Model 2 – Fuzzy approach

Finally, we used Model 2 admitting the mentioned 30% load increase and using the following parameters:

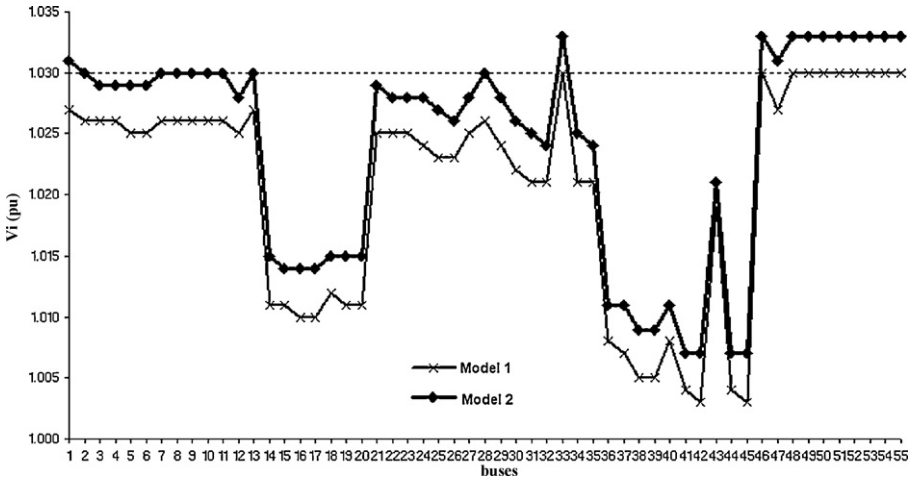

Fig. 7. Case 2 – voltage profiles obtained with Models 1 and 2.

- $FO^{\text{des}} = 104.0\,€/\text{h}$ and $\delta^{FO} = 56.0\,€/\text{h}$;
- $\delta^{V\min} = 0.02$ pu and $\delta^{V\max} = 0.02$ pu;
- $\delta_{ij}^{Sij} = 10\%$.

Taking the case of branch 1–2 as an example and using a membership function as the one illustrated in Fig. 3, if the apparent power flow in branch 1–2 is not larger than 3.5 MVA the corresponding membership function is 1.0, meaning that the crisp limit is not exceeded. However, it is admitted a tolerance of 10% on this crisp limit, meaning that the apparent power flow in this branch can go till 3.85 MVA but the corresponding membership degree decreases from 1 to 0 when going from 3.5 to 3.85 MVA. Having this in mind, Fig. 7 and Table 5 present the results obtained for this case using Model 2, namely the voltage magnitudes and the final generation and load dispatch. The capacitors connected to nodes 1 and 5 generate 2.0 and 0.5 Mvar.

These results deserve the following comments:

- in the first place, it should be mentioned that ΔPg_i^A variables related with nodes 52 and 53 are negative meaning that the initial generation values in these two buses are decreased in the final dispatch. In any case, the global generation reduction obtained in this simulation is 0.290 MW while using Model 1 the global generation reduction in buses 46, 48, 42, 53 and 55 was 0.342 MW. These values correspond to the addition of the values of the ΔPg_i^A in Tables 4 and 5, respectively;
- secondly, it should be mentioned that there is still load curtailment in node 13. The load in this node is now curtailed by 0.290 MW and this amount matches the generation reduction indicated above. The load curtailment obtained with this simulation is more reduced when compared with the load curtailment obtained with Model 1, 0.342 MW;

Table 4
Case 2 – Model 1 – final generation and load dispatch.

bus i	ΔPg_i^L MW	ΔPg_i^A MW	Pg_i MW	Qg_i Mvar	ΔPd_i^A MW	Pd_i MW	Qd_i Mvar
13	0	0	0.4	0.5	−0.342	0.828	0.401
14	–	–	–	–	0	1.089	0.358
15	–	–	–	–	0	1.089	0.358
16	–	–	–	–	0	0.545	0.179
17	–	–	–	–	0	0.545	0.179
18	–	–	–	–	0	1.089	0.358
19	–	–	–	–	0	1.089	0.358
20	–	–	–	–	0	0.545	0.179
36	–	–	–	–	0	0.281	0.136
37	–	–	–	–	0	0.176	0.085
38	–	–	–	–	0	0.176	0.085
39	–	–	–	–	0	0.112	0.054
40	–	–	–	–	0	0.281	0.136
41	–	–	–	–	0	0.176	0.085
42	–	–	–	–	0	0.112	0.054
43	0	0	1.5	−0.422	–	–	–
44	–	–	–	–	0	0.176	0.085
45	–	–	–	–	0	0.112	0.054
46	0	−0.025	0.675	0.124	–	–	–
47	0.034	0	0.034	−0.004	–	–	–
48	0	−0.002	0.798	0.262	–	–	–
49	0	0	0.25	0.04	–	–	–
50	0	0	0.25	0.034	–	–	–
51	0	0	0.25	0.034	–	–	–
52	0	−0.069	0.181	0.049	–	–	–
53	0	−0.240	0.01	0.043	–	–	–
55	0.001	−0.005	4.109	0.449	–	–	–

Table 5
Case 2 – Model 2 – final generation and load dispatch.

bus i	ΔPg_i^L MW	ΔPg_i^A MW	Pg_i MW	Qg_i Mvar	ΔPd_i^A MW	Pd_i MW	Qd_i Mvar
13	0	0	0.4	0.5	−0.290	0.88	0.426
14	–	–	–	–	0	1.089	0.358
15	–	–	–	–	0	1.089	0.358
16	–	–	–	–	0	0.545	0.179
17	–	–	–	–	0	0.545	0.179
18	–	–	–	–	0	1.089	0.358
19	–	–	–	–	0	1.089	0.358
20	–	–	–	–	0	0.545	0.179
36	–	–	–	–	0	0.281	0.136
37	–	–	–	–	0	0.176	0.085
38	–	–	–	–	0	0.176	0.085
39	–	–	–	–	0	0.112	0.054
40	–	–	–	–	0	0.281	0.136
41	–	–	–	–	0	0.176	0.085
42	–	–	–	–	0	0.112	0.054
43	0	0	1.5	−0.468	–	–	–
44	–	–	–	–	0	0.176	0.085
45	–	–	–	–	0	0.112	0.054
46	0	0	0.7	0.115	–	–	–
47	0.037	0	0.037	0.01	–	–	–
48	0	0	0.8	0.275	–	–	–
49	0	0	0.25	0.038	–	–	–
50	0	0	0.25	0.033	–	–	–
51	0	0	0.25	0.033	–	–	–
52	0	−0.040	0.21	0.048	–	–	–
53	0	−0.250	0	0.045	–	–	–
55	0	0	4.113	0.464	–	–	–

- the reduction of load curtailment by about 15% is due to the more flexible operation implicit to the Fuzzy model, namely when using soft constraints to model branch flow limits. In fact, we are now admitting that the apparent flow in branch 1–2 can exceed the crisp limit adopted in Model 1 (3.5 MW) by 10%. This allows increasing the apparent flow in branch 1–2, so that more power is transmitted to the feeder on the left of the scheme in Fig. 6, increasing the power supplied to node 13 and reducing load curtailment;
- branch losses marginally increase to 0.037 MW regarding the value obtained with Model 1. This is explained by the increase in the supplied demand and also given the corresponding increase of generated power inside the network. In this case, the power required to balance branch losses is balanced in node 47, according to the value of the ΔPg_i^L variables indicated in Table 5;
- it should be mentioned that the objective function of the Fuzzy Linear Programming problem (20), the global satisfaction degree, takes the value 0.840. This value is strongly determined by the apparent power flow limit constraint for branch 1–2. The final value of the apparent power in this branch is 3.56 MVA (3.502 MW and 0.615 Mvar). The membership value associated to 3.56 MVA is read in the membership function of this flow and it is 0.840;
- this means that it is not fully used the tolerance of 10% admitted for this apparent power flow. The more extensive use of this tolerance is prevented by other constraints in Model 2, namely the voltage limit constraints. Looking at Fig. 7, there are a number of nodes in which the voltage magnitude is larger than the crisp limit of 1.03 pu used in Model 1. In this case, we admitted a tolerance of 0.02 pu meaning that voltages could go till 1.05 pu. From Fig. 7, the voltage magnitudes in nodes 1, 33 and 46–55 partially use this tolerance;
- finally, the reduction by 15% of the load curtailment already mentioned is the main responsible for the reduction of the *FO* value in constraint (21) corresponding to the objective function (3) of the original crisp problem. This value is now 112.96 €/h which represents a reduction of 15% regarding the value of 133.76 €/h obtained with Model 1.

6. Conclusions

MicroGrids correspond to a new paradigm of distribution networks but they still face a large number of challenges. This paper was prepared as a result of the research developed in INESC Porto in the framework of a EU financed project in which some of these difficulties are addressed. The models described in this paper are able to include micro-sources and MicroGrid demand in a more natural way in electricity markets, admitting that the MicroGrid Central Controller has large responsibilities both regarding market issues (when interfacing with the Market Operator) and technical issues (when acting as the MicroGrid operator and interfacing with the DMS system of the upwards network). The described models enable MicroGrid agents to participate more actively in the electricity market, transmitting their bids to the day-ahead market and inducing their participation in a secondary adjustment market to assign ancillary services as reactive power/voltage control, active power to balance branch losses and demand curtailment. The provision of these services by MicroGrid agents will create a new flow of money and will eventually make it possible to eliminate the feed-in tariffs currently existing in several countries to pay renewable generation, given that they are responsible for an increasing share of the final end user tariffs. As a whole, these models were designed to give a further step to reach the objective initially stated – contribute to the development of the MicroGrid concept and to its widespread in the next years.

References

[1] H. Jiayi, J. Chuanwen, X. Rong, A review on distributed energy resources and MicroGrid, Renewable and Sustainable Energy Reviews 12 (2008) 2472–2483.
[2] C. Marnay, H. Asano, S. Papathanassiou, G. Strbac, Policymaking for MicroGrids, IEEE Power & Energy Magazine 6 (2008) 66–77.
[3] F. Katiraei, R. Iravani, N. Hatziargyriou, A. Dimeas, Microgrids management, IEEE Power & Energy Magazine 6 (2008) 54–65.
[4] R. Lasseter, A. Akhil, C. Marnay, J. Stephens, J. Dagle, R. Guttromson, A.S. Meliopoulous, R. Yinger, J. Eto, Integration of Distributed Energy Resources, The CERTS MicroGrid Concept, CERTS Program Office, Lawrence Berkeley National Laboratory, October 2003.

[5] J.A. Peças Lopes, J.T. Saraiva, N. Hatziargyriou, N. Jenkins, Management of MicroGrids, in: Proc. of JIEEC 2003, International Conference on the Electric Network of the Future and Distributed Generation, Bilbao, Spain, 2003, pp. 3.4/1, 3.4/16.
[6] R. Lasseter, MicroGrids and distributed generation, Journal of Energy Engineering, American Society of Civil Engineers 133 (2007) 144–149.
[7] C.L. Moreira, F.O. Resende, J.A. Peças Lopes, Using low voltage MicroGrids for service restoration, IEEE Transactions on Power Systems 22 (2007) 395–403.
[8] J.A. Peças Lopes, C.L. Moreira, A.G. Madureira, Defining control strategies for MicroGrids islanded operation, IEEE Transactions on Power Systems 21 (2006) 916–924.
[9] A. Dimeas, N. Hatziargyriou, Operation of a multiagent system for MicroGrid control, IEEE Transactions on Power Systems 20 (2005) 1447–1455.
[10] G. Celli, F. Pilo, G. Pisano, G.G. Soma, Optimal participation of a MicroGrid to the energy market with an Intelligent EMS, in: Proc. of the IPEC 2005, 7th International Power Engineering Conference, vol. 2, Singapore, 2005, pp. 663–668.
[11] J. Oyarzabal, J. Jimeno, R. Ruela, A. Engler, C. Hardt, Agent based Micro Grid management system, in: Proc. 2005 International Conference on Future Power Systems, Amsterdam, Holland, 2005.
[12] Z. Jiang, Agent-based control framework for distributed energy resources MicroGrids, in: Proc. of IAT'06, IEEE International Conference on Intelligent Agent Technology, Hong-Kong, 2006, pp. 646–652.
[13] C. Yuen, A. Oudalov, The feasibility and profitability of ancillary services provision from multi-MicroGrids, in: Proc. of the 2007 IEEE Power Tech Conference, Lausanne, Switzerland, 2007.
[14] M.H. Gomes, J.T. Saraiva, Active/reactive bid based dispatch models to be used in electricity markets, Electric Power Systems Research 78 (2008) 106–121.
[15] H.J. Zimmermann, Fuzzy Set Theory – and Its Applications, 2nd ed., Kluwer Academic Publishers, London, 1992.
[16] J.A. Peças Lopes, N. Gil, Description of a Test Network to be Used for Simulation Platform Development, MORE MICROGRIDS, WORK PACKAGE D – TD3.3, INESC Porto, July 2006.

Mário Helder Gomes was born in Mozambique in 1972. He received his licentiate, M.Sc. and Ph.D. degrees from Faculdade de Engenharia da Universidade do Porto (FEUP) in 1997, 2000 and 2007 in Electrical and Computer Engineering. In 1997 he joined the Polytechnic Institute of Tomar.

João Tomé Saraiva was born in Porto, Portugal in 1962. In 1987, 1993 and 2002 he got his M.Sc., Ph.D., and Agregado degrees in Electrical and Computer Engineering from the Faculdade de Engenharia da Universidade do Porto where he is currently Professor. In 1985 he joined INESC Porto where he was Head Researcher or collaborated in several projects related with the development of DMS systems, quality in power systems, and tariffs under a consultancy contract with the Portuguese Electricity Regulatory Agency.